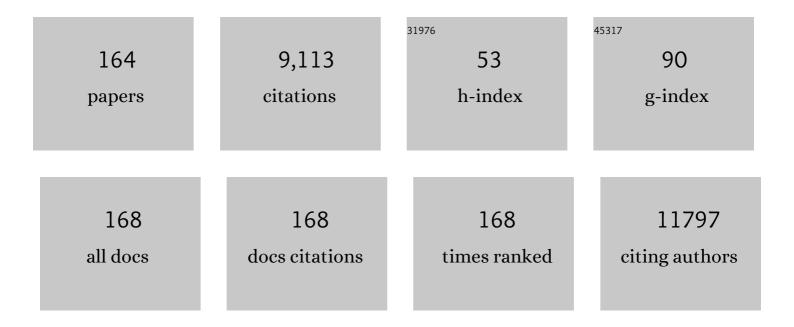
## Haisheng Qian

List of Publications by Year in descending order

Source: https://exaly.com/author-pdf/9528581/publications.pdf Version: 2024-02-01



#	Article	IF	CITATIONS
1	Mesoporousâ€Silicaâ€Coated Upâ€Conversion Fluorescent Nanoparticles for Photodynamic Therapy. Small, 2009, 5, 2285-2290.	10.0	582
2	Synthesis of Hexagonal-Phase Coreâ^'Shell NaYF <sub>4</sub> Nanocrystals with Tunable Upconversion Fluorescence. Langmuir, 2008, 24, 12123-12125.	3.5	375
3	High-Quality Luminescent Tellurium Nanowires of Several Nanometers in Diameter and High Aspect Ratio Synthesized by a Poly (Vinyl Pyrrolidone)-Assisted Hydrothermal Process. Langmuir, 2006, 22, 3830-3835.	3.5	296
4	Synthesis of Uniform Te@Carbon-Rich Composite Nanocables with Photoluminescence Properties and Carbonaceous Nanofibers by the Hydrothermal Carbonization of Glucose. Chemistry of Materials, 2006, 18, 2102-2108.	6.7	253
5	Largeâ€Scale Synthesis of Highly Luminescent Perovskiteâ€Related CsPb <sub>2</sub> Br <sub>5</sub> Nanoplatelets and Their Fast Anion Exchange. Angewandte Chemie - International Edition, 2016, 55, 8328-8332.	13.8	243
6	Singlet oxygen-induced apoptosis of cancer cells using upconversion fluorescent nanoparticles as a carrier of photosensitizer. Nanomedicine: Nanotechnology, Biology, and Medicine, 2010, 6, 486-495.	3.3	211
7	Large-Scale Fabrication of Flexible Silver/Cross-Linked Poly(vinyl alcohol) Coaxial Nanocables by a Facile Solution Approach. Journal of the American Chemical Society, 2005, 127, 2822-2823.	13.7	204
8	Synthesis and characterization of nanosized urchin-like α-Fe2O3 and Fe3O4: Microwave electromagnetic and absorbing properties. Journal of Alloys and Compounds, 2011, 509, 4320-4326.	5.5	190
9	Microwave-assisted non-aqueous route to deposit well-dispersed ZnO nanocrystals on reduced graphene oxide sheets with improved photoactivity for the decolorization of dyes under visible light. Applied Catalysis B: Environmental, 2012, 125, 425-431.	20.2	161
10	Non-catalytic CVD preparation of carbon spheres with a specific size. Carbon, 2004, 42, 761-766.	10.3	160
11	Thermoresponsive <i>in Situ</i> Forming Hydrogel with Sol–Gel Irreversibility for Effective Methicillin-Resistant <i>Staphylococcus aureus</i> Infected Wound Healing. ACS Nano, 2019, 13, 10074-10084.	14.6	160
12	Submicrometer-sized NiO octahedra: facile one-pot solid synthesis, formation mechanism, and chemical conversion into Ni octahedra with excellent microwave-absorbing properties. Journal of Materials Chemistry, 2012, 22, 17494.	6.7	156
13	Seed-mediated synthesis of NaY F <sub>4</sub> :Y b, Er <i>/</i> NaGdF <sub>4</sub> nanocrystals with improved upconversion fluorescence and MR relaxivity. Nanotechnology, 2010, 21, 125602.	2.6	149
14	Coating Colloidal Carbon Spheres with CdS Nanoparticles: Microwave-Assisted Synthesis and Enhanced Photocatalytic Activity. Langmuir, 2010, 26, 18570-18575.	3.5	149
15	Hollow mesoporous silica nanoparticles for intracellular delivery of fluorescent dye. Chemistry Central Journal, 2011, 5, 1.	2.6	147
16	Multiplex Templating Process in One-Dimensional Nanoscale: Controllable Synthesis, Macroscopic Assemblies, and Applications. Accounts of Chemical Research, 2013, 46, 1450-1461.	15.6	147
17	Magnetic-field induced formation of 1D Fe3O4/C/CdS coaxial nanochains as highly efficient and reusable photocatalysts for water treatment. Journal of Materials Chemistry, 2011, 21, 18359.	6.7	145
18	Enhanced electromagnetic characteristics of carbon nanotubes/carbonyl iron powders complex absorbers in 2–18GHz ranges. Journal of Alloys and Compounds, 2011, 509, 451-456.	5.5	145

#	Article	lF	CITATIONS
19	A novel ternary composite: fabrication, performance and application of expanded graphite/polyaniline/CoFe2O4 ferrite. Journal of Materials Chemistry, 2012, 22, 6449.	6.7	133
20	A new approach to synthesize uniform metal oxide hollow nanospheres via controlled precipitation. Nanotechnology, 2007, 18, 355602.	2.6	126
21	Flower-like Co superstructures: Morphology and phase evolution mechanism and novel microwave electromagnetic characteristics. CrystEngComm, 2012, 14, 2071.	2.6	118
22	Rolling Chain Amplification Based Signal-Enhanced Electrochemical Aptasensor for Ultrasensitive Detection of Ochratoxin A. Analytical Chemistry, 2013, 85, 10842-10849.	6.5	112
23	Attractive microwave-absorbing properties of M-BaFe12O19 ferrite. Journal of Alloys and Compounds, 2013, 557, 11-17.	5.5	108
24	Controlled synthesis of upconverting nanoparticles/ZnxCd1-xS yolk-shell nanoparticles for efficient photocatalysis driven by NIR light. Applied Catalysis B: Environmental, 2018, 224, 854-862.	20.2	105
25	Bi2S3 coated Au nanorods for enhanced photodynamic and photothermal antibacterial activities under NIR light. Chemical Engineering Journal, 2020, 397, 125488.	12.7	104
26	Interfacially Engineered Zn <sub><i>x</i></sub> Mn <sub>1–<i>x</i></sub> S@Polydopamine Hollow Nanospheres for Glutathione Depleting Photothermally Enhanced Chemodynamic Therapy. ACS Nano, 2021, 15, 11428-11440.	14.6	100
27	Nearâ€Infrared Photocatalytic Upconversion Nanoparticles/TiO <sub>2</sub> Nanofibers Assembled in Large Scale by Electrospinning. Particle and Particle Systems Characterization, 2016, 33, 248-253.	2.3	98
28	Rod-based urchin-like hollow microspheres of Bi2S3: Facile synthesis, photo-controlled drug release for photoacoustic imaging and chemo-photothermal therapy of tumor ablation. Biomaterials, 2020, 237, 119835.	11.4	95
29	A New Cubic Phase for a NaYF <sub>4</sub> Host Matrix Offering High Upconversion Luminescence Efficiency. Advanced Materials, 2015, 27, 5528-5533.	21.0	94
30	Photoinduced PEG deshielding from ROS-sensitive linkage-bridged block copolymer-based nanocarriers for on-demand drug delivery. Biomaterials, 2018, 170, 147-155.	11.4	93
31	Hybrid "Golden Fleece†Synthesis and Catalytic Performance of Uniform Carbon Nanofibers and Silica Nanotubes Embedded with a High Population of Noble-Metal Nanoparticles. Advanced Functional Materials, 2007, 17, 637-643.	14.9	92
32	Magnetite (Fe3O4) tetrakaidecahedral microcrystals: Synthesis, characterization, and micro-Raman study. Materials Characterization, 2011, 62, 148-151.	4.4	87
33	Microwave-assisted synthesis of porous CdO–CdS core–shell nanoboxes with enhanced visible-light-driven photocatalytic reduction of Cr(vi). Journal of Materials Chemistry, 2012, 22, 13895.	6.7	85
34	One-pot solution synthesis of shape-controlled copper selenide nanostructures and their potential applications in photocatalysis and photothermal therapy. Nanoscale, 2017, 9, 14512-14519.	5.6	83
35	Scalable fabrication of ZnxCd1-xS double-shell hollow nanospheres for highly efficient hydrogen production. Applied Catalysis B: Environmental, 2018, 239, 309-316.	20.2	82
36	Template-Free Synthesis of Highly Uniform α-GaOOH Spindles and Conversion to α-Ga <sub>2</sub> O <sub>3</sub> and β-Ga <sub>2</sub> O <sub>3</sub> . Crystal Growth and Design, 2008, 8, 1282-1287.	3.0	80

#	Article	IF	CITATIONS
37	Ultrastable AgBiS <sub>2</sub> Hollow Nanospheres with Cancer Cell-Specific Cytotoxicity for Multimodal Tumor Therapy. ACS Nano, 2020, 14, 14919-14928.	14.6	77
38	Folin–Ciocalteu Assay Inspired Polyoxometalate Nanoclusters as a Renal Clearable Agent for Non-Inflammatory Photothermal Cancer Therapy. ACS Nano, 2020, 14, 2126-2136.	14.6	75
39	Acetic Acid-Assisted Solution Process for Growth of Complex Copper Sulfide Microtubes Constructed by Hexagonal Nanoflakes. Chemistry of Materials, 2006, 18, 2012-2015.	6.7	74
40	Precisely photothermal controlled releasing of antibacterial agent from Bi2S3 hollow microspheres triggered by NIR light for water sterilization. Chemical Engineering Journal, 2020, 381, 122630.	12.7	74
41	Selective preparation and enhanced microwave electromagnetic characteristics of polymorphous ZnO architectures made from a facile one-step ethanediamine-assisted hydrothermal approach. CrystEngComm, 2013, 15, 1314.	2.6	73
42	Synthesis of copper/cross-linked poly(vinyl alcohol) (PVA) nanocables via a simple hydrothermal route. Journal of Materials Chemistry, 2006, 16, 101-105.	6.7	72
43	Bimetallic oxide Cu1.5Mn1.5O4 cage-like frame nanospheres with triple enzyme-like activities for bacterial-infected wound therapy. Nano Today, 2022, 43, 101380.	11.9	70
44	Titanium Dioxide/Upconversion Nanoparticles/Cadmium Sulfide Nanofibers Enable Enhanced Full‧pectrum Absorption for Superior Solar Light Driven Photocatalysis. ChemSusChem, 2016, 9, 1449-1454.	6.8	67
45	Biomimetic copper single-atom nanozyme system for self-enhanced nanocatalytic tumor therapy. Nano Research, 2022, 15, 7320-7328.	10.4	66
46	One-pot solvothermal synthesis of multi-shelled α-Fe2O3 hollow spheres with enhanced visible-light photocatalytic activity. Journal of Alloys and Compounds, 2013, 551, 440-443.	5.5	64
47	Synthesis of tellurium nanowires and their transport property. Materials Chemistry and Physics, 2009, 113, 523-526.	4.0	58
48	ZnO/ZnFe <sub>2</sub> O <sub>4</sub> Magnetic Fluorescent Bifunctional Hollow Nanospheres: Synthesis, Characterization, and Their Optical/Magnetic Properties. Journal of Physical Chemistry C, 2010, 114, 17455-17459.	3.1	58
49	Growth of ZnO Crystals with Branched Spindles and Prismatic Whiskers from Zn3(OH)2V2O7·H2O Nanosheets by a Hydrothermal Route. Crystal Growth and Design, 2005, 5, 935-939.	3.0	56
50	Tumor acidity-activatable TAT targeted nanomedicine for enlarged fluorescence/magnetic resonance imaging-guided photodynamic therapy. Biomaterials, 2017, 133, 165-175.	11.4	56
51	Construction of ZnxCd1â^'xS/Bi2S3 composite nanospheres with photothermal effect for enhanced photocatalytic activities. Journal of Colloid and Interface Science, 2019, 546, 303-311.	9.4	56
52	Anti-inflammatory catecholic chitosan hydrogel for rapid surgical trauma healing and subsequent prevention of tumor recurrence. Chinese Chemical Letters, 2020, 31, 1807-1811.	9.0	56
53	Charge reversal induced colloidal hydrogel acts as a multi-stimuli responsive drug delivery platform for synergistic cancer therapy. Materials Horizons, 2019, 6, 711-716.	12.2	55
54	Anti-biofouling double-layered unidirectional scaffold for long-term solar-driven water evaporation. Journal of Materials Chemistry A, 2019, 7, 16696-16703.	10.3	55

#	Article	IF	CITATIONS
55	Dispersibility, Stabilization, and Chemical Stability of Ultrathin Tellurium Nanowires in Acetone:Â Morphology Change, Crystallization, and Transformation into TeO2in Different Solvents. Langmuir, 2007, 23, 3409-3417.	3.5	54
56	A Donor–Acceptor Conjugated Polymer with Alternating Isoindigo Derivative and Bithiophene Units for Near-Infrared Modulated Cancer Thermo-Chemotherapy. ACS Applied Materials & Interfaces, 2016, 8, 19312-19320.	8.0	54
57	Large scale synthesis of uniform silver@carbon rich composite (carbon and cross-linked PVA) sub-microcables by a facile green chemistry carbonization approach. Chemical Communications, 2006, , 793.	4.1	53
58	Upconversion nanoparticles@AgBiS2 core-shell nanoparticles with cancer-cell-specific cytotoxicity for combined photothermal and photodynamic therapy of cancers. Bioactive Materials, 2022, 17, 71-80.	15.6	52
59	Morphology dependence of static magnetic and microwave electromagnetic characteristics of polymorphic Fe <sub>3</sub> O <sub>4</sub> nanomaterials. Journal of Materials Research, 2011, 26, 1639-1645.	2.6	51
60	A general approach for synthesis of a family of functional inorganic nanotubes using highly active carbonaceous nanofibres as templates. Journal of Materials Chemistry, 2009, 19, 1037-1042.	6.7	50
61	Microwave-assisted route to fabricate coaxial ZnO/C/CdS nanocables with enhanced visible light-driven photocatalytic activity. CrystEngComm, 2012, 14, 7686.	2.6	50
62	Facile synthesis of Ag2WO4/AgCl nanorods for excellent photocatalytic properties. Materials Letters, 2013, 91, 129-132.	2.6	50
63	Facile synthesis of CdS/C core–shell nanospheres with ultrathin carbon layer for enhanced photocatalytic properties and stability. Applied Surface Science, 2016, 362, 126-131.	6.1	49
64	PEGylated rhenium nanoclusters: a degradable metal photothermal nanoagent for cancer therapy. Chemical Science, 2019, 10, 5435-5443.	7.4	49
65	Redox-Responsive Polyphosphoester-Based Micellar Nanomedicines for Overriding Chemoresistance in Breast Cancer Cells. ACS Applied Materials & Interfaces, 2015, 7, 26315-26325.	8.0	48
66	PVA-Assisted Hydrothermal Synthesis of Copper@Carbonaceous Submicrocables:  Thermal Stability, and Their Conversion into Amorphous Carbonaceous Submicrotubes. Journal of Physical Chemistry C, 2007, 111, 2490-2496.	3.1	47
67	Enhanced electromagnetic characteristics of porous iron particles made by a facile corrosion technique. Materials Chemistry and Physics, 2012, 132, 563-569.	4.0	47
68	Novel doxorubicin loaded PEGylated cuprous telluride nanocrystals for combined photothermal-chemo cancer treatment. Colloids and Surfaces B: Biointerfaces, 2017, 152, 449-458.	5.0	46
69	Controlled synthesis of upconverting nanoparticles/CuS yolk–shell nanoparticles for <i>in vitro</i> synergistic photothermal and photodynamic therapy of cancer cells. Journal of Materials Chemistry B, 2017, 5, 9487-9496.	5.8	44
70	Design of Tumor Acidity-Responsive Sheddable Nanoparticles for Fluorescence/Magnetic Resonance Imaging-Guided Photodynamic Therapy. Theranostics, 2017, 7, 1290-1302.	10.0	44
71	Unique Upconversion Core–Shell Nanoparticles with Tunable Fluorescence Synthesized by a Sequential Growth Process. Advanced Materials Interfaces, 2016, 3, 1500649.	3.7	43
72	Sequential Growth of NaYF <sub>4</sub> :Yb/Er@NaGdF <sub>4</sub> Nanodumbbells for Dual-Modality Fluorescence and Magnetic Resonance Imaging. ACS Applied Materials & Interfaces, 2017, 9, 9226-9232.	8.0	41

#	Article	IF	CITATIONS
73	Synthesis of Mesoporous SiO <sub>2</sub> @TiO <sub>2</sub> Core/Shell Nanospheres with Enhanced Photocatalytic Properties. Particle and Particle Systems Characterization, 2013, 30, 306-310.	2.3	39
74	Multicolor polystyrene nanospheres tagged with up-conversion fluorescent nanocrystals. Nanotechnology, 2008, 19, 255601.	2.6	38
75	Facile synthesis of tremelliform Co0.85Se nanosheets: An efficient catalyst for the decomposition of hydrazine hydrate. Applied Catalysis B: Environmental, 2012, 119-120, 139-145.	20.2	38
76	Stable gadolinium based nanoscale lyophilized injection for enhanced MR angiography with efficient renal clearance. Biomaterials, 2018, 158, 74-85.	11.4	37
77	Te@Cross-Linked PVA Coreâ^'Shell Structures Synthesized by a One-Step Synergistic Softâ^'Hard Template Process. Crystal Growth and Design, 2006, 6, 607-611.	3.0	36
78	Grinding speed dependence of microstructure, conductivity, and microwave electromagnetic and absorbing characteristics of the flaked Fe particles. Journal of Materials Research, 2011, 26, 682-688.	2.6	36
79	Monitoring and removal of trace heavy metal ions via fluorescence resonance energy transfer mechanism: In case of silver ions. Chemical Engineering Journal, 2019, 375, 121927.	12.7	36
80	Mesoporous silica nanospheres decorated with CdS nanocrystals for enhanced photocatalytic and excellent antibacterial activities. Nanoscale, 2013, 5, 6327.	5.6	33
81	Large‣cale Synthesis of Highly Luminescent Perovskiteâ€Related CsPb <sub>2</sub> Br <sub>5</sub> Nanoplatelets and Their Fast Anion Exchange. Angewandte Chemie, 2016, 128, 8468-8472.	2.0	33
82	Facile microemulsion route to coat carbonized glucose on upconversion nanocrystals as high luminescence and biocompatible cell-imaging probes. Nanotechnology, 2010, 21, 315105.	2.6	32
83	Facile Clâ^'-mediated hydrothermal synthesis of large-scale Ag nanowires from AgCl hydrosol. CrystEngComm, 2013, 15, 2598.	2.6	30
84	Mesoporous-silica-coated upconversion nanoparticles loaded with vitamin B12 for near-infrared-light mediated photodynamic therapy. Materials Letters, 2016, 167, 205-208.	2.6	30
85	PEGylated hyperbranched polyphosphoester based nanocarriers for redox-responsive delivery of doxorubicin. Biomaterials Science, 2016, 4, 412-417.	5.4	30
86	Expanded graphite/polyaniline electrical conducting composites: Synthesis, conductive and dielectric properties. Materials Letters, 2010, 64, 1313-1315.	2.6	27
87	Mesoporous silica-coated NaYF4 nanocrystals: facile synthesis, in vitro bioimaging and photodynamic therapy of cancer cells. RSC Advances, 2012, 2, 12263.	3.6	27
88	Phototherapy Using a Fluoroquinolone Antibiotic Drug to Suppress Tumor Migration and Proliferation and to Enhance Apoptosis. ACS Nano, 2022, 16, 4917-4929.	14.6	27
89	Polyphosphoester-Based Nanoparticles with Viscous Flow Core Enhanced Therapeutic Efficacy by Improved Intracellular Drug Release. ACS Applied Materials & Interfaces, 2014, 6, 16174-16181.	8.0	26
90	Sequential growth of sandwiched NaYF4:Yb/Er@NaYF4:Yb@NaNdF4:Yb core–shell–shell nanoparticles for photodynamic therapy. Applied Surface Science, 2015, 357, 2408-2414.	6.1	26

#	Article	IF	CITATIONS
91	Sequential growth of CaF <sub>2</sub> :Yb,Er@CaF <sub>2</sub> :Cd nanoparticles for efficient magnetic resonance angiography and tumor diagnosis. Biomaterials Science, 2017, 5, 2403-2415.	5.4	26
92	Copperâ€based nanomaterials for cancer theranostics. Wiley Interdisciplinary Reviews: Nanomedicine and Nanobiotechnology, 2022, 14, e1797.	6.1	26
93	Facile synthesis of UCNPs/Zn x Cd 1-x S nanocomposites excited by near-infrared light for photochemical reduction and removal of Cr(VI). Chinese Journal of Catalysis, 2018, 39, 1240-1248.	14.0	25
94	Magnetically Recyclable Fe <sub>3</sub> O <sub>4</sub> @Zn <sub><i>x</i></sub> Cd <sub>1–<i>x</i></sub> S Core–Shell Microspheres for Visible Light-Mediated Photocatalysis. Langmuir, 2018, 34, 9264-9271.	3.5	25
95	Polyoxometalate nanoclusters: A potential preventative and therapeutic drug for inflammatory bowel disease. Chemical Engineering Journal, 2021, 416, 129137.	12.7	25
96	Facile Synthesis of Upconverting Nanoparticles/Zinc Oxide Core–Shell Nanostructures with Large Lattice Mismatch for Infrared Triggered Photocatalysis. Particle and Particle Systems Characterization, 2017, 34, 1600222.	2.3	24
97	ICG@ZIF-8/PDA/Ag composites as chemo-photothermal antibacterial agents for efficient sterilization and enhanced wound disinfection. Journal of Materials Chemistry B, 2021, 9, 9961-9970.	5.8	24
98	Facile synthesis of GdBO3 spindle assemblies and microdisks as versatile host matrices for lanthanide doping. CrystEngComm, 2012, 14, 3959.	2.6	23
99	Upconversion nanoparticles modified with aminosilanes as carriers of DNA vaccine for foot-and-mouth disease. Applied Microbiology and Biotechnology, 2012, 95, 1253-1263.	3.6	22
100	Mesoporous NiS <sub>2</sub> nanospheres as a hydrophobic anticancer drug delivery vehicle for synergistic photothermal–chemotherapy. Journal of Materials Chemistry B, 2019, 7, 143-149.	5.8	22
101	Controlled Synthesis of the Poly(N-methylaniline)/Zn0.6Mn0.2Ni0.2Fe2O4 Composites and Its Electrical-Magnetic Property. Journal of Physical Chemistry C, 2010, 114, 6712-6717.	3.1	19
102	Silica/ultrasmall Ag composite microspheres: facile synthesis, characterization and antibacterial and catalytic performance. CrystEngComm, 2014, 16, 2365-2370.	2.6	19
103	Photocatalytic studies of CdS nanoparticles assembled on carbon microsphere surfaces with different interface structures: from amorphous to graphite-like carbon. CrystEngComm, 2012, 14, 4507.	2.6	18
104	Facile synthesis of uniform ZnxCd1â^'xS alloyed hollow nanospheres for improved photocatalytic activities. Journal of Materials Science: Materials in Electronics, 2014, 25, 4103-4109.	2.2	18
105	Fabrication of Zinc Oxide Composite Microfibers for Nearâ€Infraredâ€Lightâ€Mediated Photocatalysis. ChemCatChem, 2017, 9, 3611-3617.	3.7	17
106	Ag nanoparticles decorated hybrid microspheres for superior antibacterial properties. Materials Letters, 2020, 262, 127057.	2.6	17
107	A tumour microenvironment-mediated Bi <sub>2â~'<i>x</i></sub> Mn <sub><i>x</i></sub> O <sub>3</sub> hollow nanospheres <i>via</i> glutathione depletion for photothermal enhanced chemodynamic collaborative therapy. Journal of Materials Chemistry B, 2022, 10, 3452-3461.	5.8	17
108	Electrical and microwave absorbing properties of polypyrrole synthesized by optimum strategy. Journal of Applied Polymer Science, 2013, 127, 4273-4279.	2.6	16

#	Article	IF	CITATIONS
109	Decoration of upconversion nanoparticles@mSiO2 core–shell nanostructures with CdS nanocrystals for excellent infrared light triggered photocatalysis. RSC Advances, 2016, 6, 54241-54248.	3.6	16
110	Decoration of ZnO nanocrystals on the surface of shuttle-shaped Mn2O3 and its magnetic-optical properties. CrystEngComm, 2010, 12, 2687.	2.6	15
111	Facile synthesis of β-NaGdF <sub>4</sub> :Yb/Er@CaF <sub>2</sub> nanoparticles with enhanced upconversion fluorescence and stability via a sequential growth process. CrystEngComm, 2015, 17, 5900-5905.	2.6	15
112	<scp>dl</scp> -Menthol Loaded Polypyrrole Nanoparticles as a Controlled Diclofenac Delivery Platform for Sensitizing Cancer Cells to Photothermal Therapy. ACS Applied Bio Materials, 2019, 2, 848-855.	4.6	15
113	Recent Development on Controlled Synthesis of Mnâ€Based Nanostructures for Bioimaging and Cancer Therapy. Advanced Therapeutics, 2021, 4, 2100018.	3.2	15
114	A multifunctional composite hydrogel as an intrinsic and extrinsic coregulator for enhanced therapeutic efficacy for psoriasis. Journal of Nanobiotechnology, 2022, 20, 155.	9.1	15
115	Enhanced microwave absorption properties of Fe nanotubes fabricated by a facile gas bubble-engaged assembly technique. Micro and Nano Letters, 2011, 6, 722.	1.3	14
116	TiO2 composite nanotubes embedded with CdS and upconversion nanoparticles for near infrared light driven photocatalysis. Chinese Journal of Catalysis, 2017, 38, 1851-1859.	14.0	13
117	Synthesis of uniform carbon@silica nanocables and luminescent silica nanotubes with well controlled inner diameters. Nanotechnology, 2006, 17, 5995-5999.	2.6	12
118	Facile synthesis of magnetic metal (Mn, Co, Fe, and Ni) oxide nanosheets. Materials Letters, 2010, 64, 1095-1098.	2.6	12
119	Self-assembly of TiO2 composite microspheres: Facile synthesis, characterization and photocatalytic activities. CrystEngComm, 2012, 14, 7118.	2.6	12
120	Hydrothermal-assisted crystallization for the synthesis of upconversion nanoparticles/CdS/TiO <sub>2</sub> composite nanofibers by electrospinning. CrystEngComm, 2016, 18, 6013-6018.	2.6	12
121	Recent Development on Controlled Synthesis of Metal Sulfides Hollow Nanostructures via Hard Template Engaged Strategy: A Miniâ€Review. Chemical Record, 2020, 20, 882-892.	5.8	12
122	Inhibition of Murine Bladder Cancer Cell Growth In Vitro by Photocontrollable siRNA Based on Upconversion Fluorescent Nanoparticles. PLoS ONE, 2014, 9, e112713.	2.5	12
123	Large-Scale Synthesis of Flexible Gold/Cross-Linked-PVA Sub-Microcables and Cross-Linked-PVA Tubes/Fibers by Using Templating Approaches Based on Silver/Cross-Linked-PVA Sub-Microcables. Chemistry - A European Journal, 2006, 12, 3320-3324.	3.3	11
124	Large-Scale Ligand-Free Synthesis of Homogeneous Core–Shell Quantum-Dot-Modified Cs <sub>4</sub> PbBr <sub>6</sub> Microcrystals. Inorganic Chemistry, 2019, 58, 10620-10624.	4.0	11
125	Synthesis, Characterization, and In Vitro Drug Delivery of Chitosan-Silica Hybrid Microspheres for Bone Tissue Engineering. Journal of Nanomaterials, 2019, 2019, 1-7.	2.7	11
126	Synthesis of CoSnS <sub>2</sub> hollow nanocubes with NIR-enhanced chemodynamic therapy and glutathione depletion for combined cancer therapy. Materials Chemistry Frontiers, 2022, 6, 1522-1532.	5.9	11

#	Article	IF	CITATIONS
127	Expanded graphite/cobalt ferrite/polyaniline ternary composites: Fabrication, properties, and potential applications. Journal of Materials Research, 2011, 26, 2683-2690.	2.6	10
128	Synthesis of streptavidin-conjugated magnetic nanoparticles for DNA detection. Journal of Nanoparticle Research, 2013, 15, 1.	1.9	10
129	Highly Active Zinc Sulfide Composite Microspheres: A Versatile Template for Synthesis of a Family of Hollow Nanostructures of Sulfides. Langmuir, 2020, 36, 1523-1529.	3.5	10
130	Synthesis of sea-urchin-like Bi2S3 hollow microspheres for highly efficient removal of Ag+ with extremely low acidity. Applied Surface Science, 2020, 515, 146130.	6.1	10
131	KMnF3 nanowires and nanoparticles: Selected synthesis, characterization and magnetic properties. Materials Letters, 2017, 196, 145-148.	2.6	9
132	Reprogrammable Untethered Actuator for Soft Bioâ€Inspired Robots. Advanced Intelligent Systems, 2021, 3, 2000146.	6.1	9
133	A new trick (hydroxyl radical generation) of an old vitamin (B <sub>2</sub> ) for near-infrared-triggered photodynamic therapy. RSC Advances, 2016, 6, 102647-102656.	3.6	8
134	<p>Association of atorvastatin with the risk of hepatotoxicity: a pilot prescription sequence symmetry analysis</p> . Therapeutics and Clinical Risk Management, 2019, Volume 15, 803-810.	2.0	8
135	Sequential Growth of High Quality Sub-10 nm Core–Shell Nanocrystals: Understanding the Nucleation and Growth Process Using Dynamic Light Scattering. Langmuir, 2019, 35, 489-494.	3.5	8
136	Amine salts assisted controllable synthesis of the YVO4:Eu3+ nanocrystallines and their luminescence properties. Physica B: Condensed Matter, 2019, 557, 1-5.	2.7	8
137	Fabrication of Wearable Hydrogel Sensors With Simple Ionic-Digital Conversion and Inherent Water Retention. IEEE Sensors Journal, 2021, 21, 6802-6810.	4.7	8
138	Green Strategy to Develop Novel Drug-Containing Poly (ε-Caprolactone)-Chitosan-Silica Xerogel Hybrid Fibers for Biomedical Applications. Journal of Nanomaterials, 2020, 2020, 1-6.	2.7	8
139	External Fieldâ€Driven Untethered Microrobots for Targeted Cargo Delivery. Advanced Materials Technologies, 2022, 7, .	5.8	8
140	Polyacrylamide/Zn0.4Ni0.5Cu0.1Fe2O4 nanocomposites: Synthesis, characterization and electromagnetic properties. Materials Chemistry and Physics, 2010, 124, 1039-1045.	4.0	7
141	Silica-based hybrid microspheres: synthesis, characterization and wastewater treatment. RSC Advances, 2013, 3, 25620.	3.6	7
142	Recent Advances in Controlled Synthesis of Upconversion Nanoparticles and Semiconductor Heterostructures. Chemical Record, 2020, 20, 2-9.	5.8	7
143	One-pot synthesis of biocompatible Te@phenol formaldehyde resin core–shell nanowires with uniform size and unique fluorescent properties by a synergized soft–hard template process. Nanotechnology, 2010, 21, 495602.	2.6	6
144	Facile synthesis of Ag@TiO2 (B) hierarchical core–shell nanowires: facile synthesis, growth mechanism and photocatalytic and antibacterial applications. Journal of Materials Science: Materials in Electronics, 2015, 26, 5753-5760.	2.2	6

#	Article	IF	CITATIONS
145	A Facile and Generic Strategy to Synthesize Large-Scale Carbon Nanotubes. Journal of Nanomaterials, 2010, 2010, 1-5.	2.7	5
146	Facile synthesis and properties of spherical assemblies of NaYF4 nanocrystals with consistent crystalline orientation. CrystEngComm, 2011, 13, 7009.	2.6	5
147	Preparation of Highly Photoluminescent CdTe Nanocrystals in a Mixing Alkali Medium. Chemistry Letters, 2016, 45, 535-537.	1.3	5
148	Epitaxial growth of ultrathin layers on the surface of sub-10Ânm nanoparticles: the case of β-NaGdF <sub>4</sub> :Yb/Er@NaDyF <sub>4</sub> nanoparticles. RSC Advances, 2018, 8, 12944-12950.	3.6	5
149	UCNPs@Zn <sub>0.5</sub> Cd <sub>0.5</sub> S Core-Shell and Yolk-Shell Nanostructures: Selective Synthesis, Characterization, and Near-Infrared-Mediated Photocatalytic Reduction of Cr(VI). Journal of Nanomaterials, 2018, 2018, 1-9.	2.7	5
150	The association between BACH1 polymorphisms and anti-tuberculosis drug-induced hepatotoxicity in a Chinese cohort. Infection, Genetics and Evolution, 2018, 66, 217-221.	2.3	5
151	Autophagic blockage by bismuth sulfide nanoparticles inhibits migration and invasion of HepG2 cells. Nanotechnology, 2020, 31, 465102.	2.6	5
152	Can t-Te Nanowires Really Give Blue-Violet Emission? Reply to Comment on High-Quality Luminescent Tellurium Nanowires of Several Nanometers in Diameter and High Aspect Ratio Synthesized by a Poly(Vinyl Pyrrolidone)-Assisted Hydrothermal Process. Langmuir, 2008, 24, 8393-8394.	3.5	4
153	Controlled fabrication and electrical-magnetic properties of Poly(OT-co-AN)/Ba0.8La0.2Al2Fe10O19 composites. Science China Technological Sciences, 2012, 55, 6-15.	4.0	4
154	Facile synthesis of the SiO <sub>2</sub> /Au hybrid microspheres for excellent catalytic performance. Journal of Materials Research, 2014, 29, 1417-1423.	2.6	4
155	PPh3-Mediated [3+2] Cycloaddition Reaction between Bis-Substituted Allenoate and N-Tosylaldimines to Construct 2-Pyrrolines. Synlett, 2018, 29, 1244-1248.	1.8	4
156	Facile Synthesis of Thermo-Sensitive Composite Hydrogel with Well Dispersed Ag Nanoparticles for Application in Superior Antibacterial Infections. Journal of Biomedical Nanotechnology, 2021, 17, 1148-1159.	1.1	4
157	Core-Shell Nanostructures: Modeling, Fabrication, Properties, and Applications. Journal of Nanomaterials, 2012, 2012, 1-2.	2.7	3
158	Small lanthanide-doped Sr2YbF7 nanocrystals: Upconversion fluorescence and upconversion-driven photodegradation. Optical Materials, 2018, 86, 537-544.	3.6	3
159	Au nanocluster-modulated macrophage polarization and synoviocyte apoptosis for enhanced rheumatoid arthritis treatment. Journal of Materials Chemistry B, 2022, 10, 4789-4799.	5.8	2
160	Enhanced therapeutic efficacy with hydrophobic polyphosphoester-based nanoparticles via improved intracellular drug release. Journal of Controlled Release, 2015, 213, e117.	9.9	1
161	Facile synthesis of Ag@SiO2 core–shell nanowires on large scale. Journal of Materials Science: Materials in Electronics, 2015, 26, 1602-1607.	2.2	1
162	Research of special carbon nanobeads supported Pt catalyst for fuel cell through high temperature pyrolysis and deposition from novel phthalocyanine. Science Bulletin, 2004, 49, 447-451.	1.7	0

#	Article	IF	CITATIONS
163	Hydrothermal Synthesis of TiO2 Hollow Nanospheres via Self-Assembly Process. Asian Journal of Chemistry, 2013, 25, 7927-7930.	0.3	0
164	Facile Synthesis of AgCl Hollow Nanospheres for Enhanced Photocatalytic Properties. American Journal of Engineering and Applied Sciences, 2015, 8, 285-290.	0.6	0